Earthquakes and plastic deformation of anhydrous slab mantle in double Wadati-Benioff zones

Bruno Reynard, Junichi Nakajima, Hitoshi Kawakatsu

Earthquakes and plastic deformation of anhydrous slab mantle in double Wadati-Benioff zones

Bruno Reynard,[1,2] Junichi Nakajima,[3] and Hitoshi Kawakatsu[2]

Received 14 September 2010; revised 3 November 2010; accepted 9 November 2010; published 29 December 2010.

[1] Double Wadati-Benioff seismic zones (DSZ) with two parallel planes of seismicity separated by 15–30 km are a global feature of subduction zones in the 50–200 km depth range. Upper plane seismicity is generally attributed to dehydration of the oceanic crust but the origin of the lower seismicity plane is debated. Serpentine or hydrous-phase dehydration embrittlement is a commonly advocated mechanism that implies significant slab mantle hydration. High-resolution seismic tomography revealed low seismic velocities in the lower seismicity plane that are better explained by seismic anisotropy of anhydrous deformed peridotites than by serpentinization. Earthquakes correlate with anisotropic planar shear zones and favor a shear instability mechanism as the cause of lower plane seismicity without requiring the presence of water in the center of subducting slabs. The contribution of the subducted lithospheric mantle to the water budget of subduction zones is thus likely limited to the first 2–3 kilometers beneath oceanic crust. **Citation:** Reynard, B., J. Nakajima, and H. Kawakatsu (2010), Earthquakes and plastic deformation of anhydrous slab mantle in double Wadati-Benioff zones, *Geophys. Res. Lett.*, *37*, L24309, doi:10.1029/2010GL045494.

1. Introduction

[2] In the mantle surrounding the lower seismic plane of DSZ [*Hasegawa et al.*, 1978], high-resolution seismic tomography of the subduction of the Pacific beneath N–E Japan [*Nakajima et al.*, 2009a, 2009b] highlights low seismic-velocity where the velocity decrease is much higher for compressional-wave (V_P) than for shear-wave velocities (V_S) (Figure 1), yielding V_P/V_S ratio below 1.73. Velocity decrease in the shallow mantle is usually attributed to serpentinization. Serpentinization would provide the link with seismicity via dehydration embrittlement [*Peacock*, 2001] but implies that the V_P/V_S ratio increases above 1.73 [*Christensen*, 2004]. Alternatively, we argue that seismicity and the associated mantle deformation can be the cause of the low velocities and V_P/V_S ratio rather than the result of serpentinite dehydration.

[3] Deformation results in seismic anisotropy that can affect the tomographic images obtained from double-difference tomography using arrival-time data from local events with limited ray coverage. Seismic rays used to image the lower seismic plane are clustered around specific directions (Figure 1) and sample specific orientations in the anisotropic velocity tensor. At shallower depths, seismic rays have more distributed orientations (Figure 1), resulting in smaller variations of velocities around the isotropic values.

[4] Anisotropic rock models were compared with tomographic velocities. A model was constructed that takes into account regional deformation of the lithospheric mantle inherited from oceanic extension at the ridge and localized-deformation overprint induced by earthquakes in the lower plane of DSZ. The deformed, anisotropic and anhydrous slab-mantle model was compared with the tomographic observations, and used to discuss the origin of lower plane seismicity and water recycling in subduction.

2. Rock seismic anisotropy

[5] Seismic anisotropy was calculated for mantle rocks whose component mineral elastic constants and crystal-preferred orientations (CPO) are known using the CareWare package [*Mainprice*, 1990]. Two anisotropic peridotite models were used, a pure A-type fabric olivine [*Jung et al.*, 2006] and a 70% olivine-30% orthopyroxene peridotite for the lithosphere [*Pera et al.*, 2003]. A serpentinite model appropriate for the subduction zone context was used [*Bezacier et al.*, 2010]. V_P and V_S were calculated for about 900 directions and used to construct the stereographic projection and plots (Figures 2 and 3). Values for minerals and rocks were computed with elastic constants measured at ambient conditions (Figure 2a). The effects of varying pressure and temperature were calculated for the isotropic models of olivine [*Abramson et al.*, 1997; *Isaak*, 1992] and orthopyroxene [*Jackson et al.*, 2007; *Webb and Jackson*, 1993], and serpentine [*Reynard et al.*, 2007].

[6] Anisotropy in mantle rocks results in large variation of V_P when compared with V_{S1} (the fastest V_S branch) whereas changing composition results in a diagonal distribution with a slope close to 1.73, the average V_P/V_S ratio of mantle rocks [*Christensen*, 2004] (Figure 2a). Changing pressure or temperature also yields diagonal distribution with slope near 1–1.5. The average lithospheric model [*Pera et al.*, 2003] covers a broader velocity range than the pure olivine aggregate [*Jung et al.*, 2006] because of the contribution from orthopyroxene. The larger variability of V_P (1 km.s^{-1} for the average and up to 1.5 km.s^{-1} in individual samples [*Pera et al.*, 2003]) when compared with V_S (0.27 km.s^{-1}) leads to a horizontal distribution of V_P-V_S couples. The range of V_P and V_S covered by the serpentinite model is much wider and at lower velocities than peridotite because of the large elastic anisotropy of antigorite [*Bezacier et al.*, 2010]. Partially serpentinized peridotites will have intermediate velocities between those of dry rocks and pure serpentinite. Hydration

[1] Laboratoire de Sciences de la Terre, UMR 5570, Université de Lyon, CNRS, Ecole Normale Supérieure de Lyon, Lyon, France.
[2] Earthquake Research Institute, University of Tokyo, Tokyo, Japan.
[3] Research Center for Prediction of Earthquakes and Volcanic Eruptions, Graduate School of Science, Tohoku University, Sendai, Japan.

0094-8276/10/2010GL045494

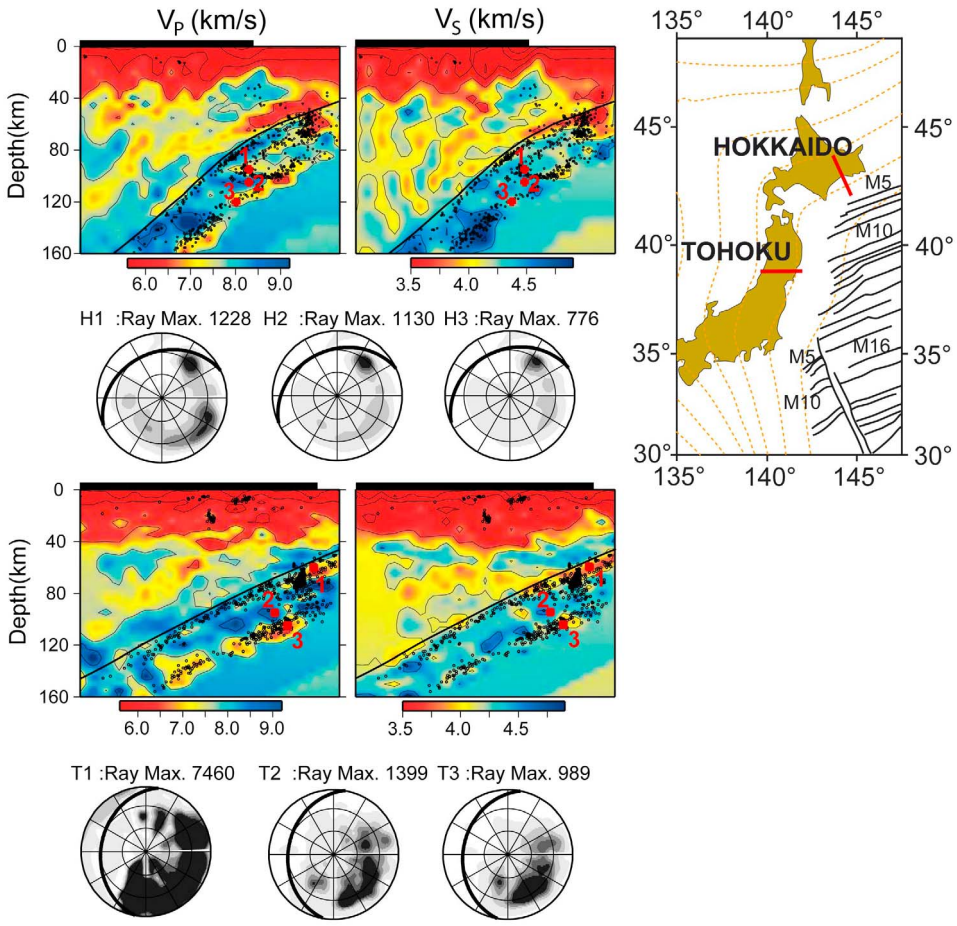

Figure 1. Tomographic cross sections of the Pacific subduction under N–E Japan. Low-velocity patches with higher velocity contrast for V_P than for V_S occur along the lower seismicity plane (hypocenters: black dots), about 20–30 km beneath the slab surface (black line) both in (top) Hokkaido and (bottom) Tohoku. Orientations of the seismic rays used in tomographic reconstruction (shown as lower hemisphere stereographic projections) are distributed for areas well above the lower seismicity plane (point T1) whereas they cluster around specific directions when approaching it (points T2, T3, H2, and H3). The horizontal high-seismicity plane with low-V_P anomaly (point H1) is associated with the source and aftershock propagation zone of the 1993 Kushiro-oki earthquake.

of the mantle should result in much larger V_P-V_S variations than anisotropy in dry mantle rocks.

3. Comparison with tomography

[7] Three regions were distinguished for comparing tomographic V_P-V_S couples with the anisotropic model mantle rocks (Figures 2 and S1 of the auxiliary material): the mantle wedge, the lithospheric mantle between the oceanic crust and lower plane, and the lithospheric mantle around the lower seismicity plane.[1] The oceanic crust was removed from the analysis. With a resolution of at best 5 km, such a thin layer as the oceanic crust (typically 7 km) may be imperfectly separated from the wedge and slab lithospheric mantle. Velocities obtained from arrival-time data inversion are affected by numerical noise as residuals of the fitting procedures. They were smoothed using as an estimator the running average of a gliding window whose optimum size was defined by minimizing the sum of variance and bias (monotonically decreasing and increasing functions with increasing window size, respectively; Figure S2).

[8] In the lower seismicity plane (Figure 2b), the observed velocity distribution matches that of the anisotropic lithospheric peridotite [*Pera et al.*, 2003], and linear regression of V_P against V_S has a nearly horizontal slope illustrating the dominance of anisotropic effects. The full range of anisotropy of dry lithospheric peridotites provides a sufficient explanation for the low velocities and V_P/V_S ratios around the lower plane. Anisotropy in olivine aggregate alone is not strong enough to match the observed velocity range and contribution from pyroxene is essential. In this region, the effect of pressure on velocities (2–5 GPa) partly compensate those of temperature (500–800°C), and observed velocities fall just below to those calculated at ambient conditions for peridotite. Contribution from serpentinites cannot be ruled out but is not a necessary condition for matching the observations.

[9] In the mantle wedge (Figure 2c), V_P and V_S cover a much larger range of values than in the lower plane because effects of the wide temperature range (up to 1000 K from the cold nose near to trench to the molten region under the volcanic arc) dominate, resulting in expected variations of

[1]Auxiliary materials are available in the HTML. doi:10.1029/2010GL045494.

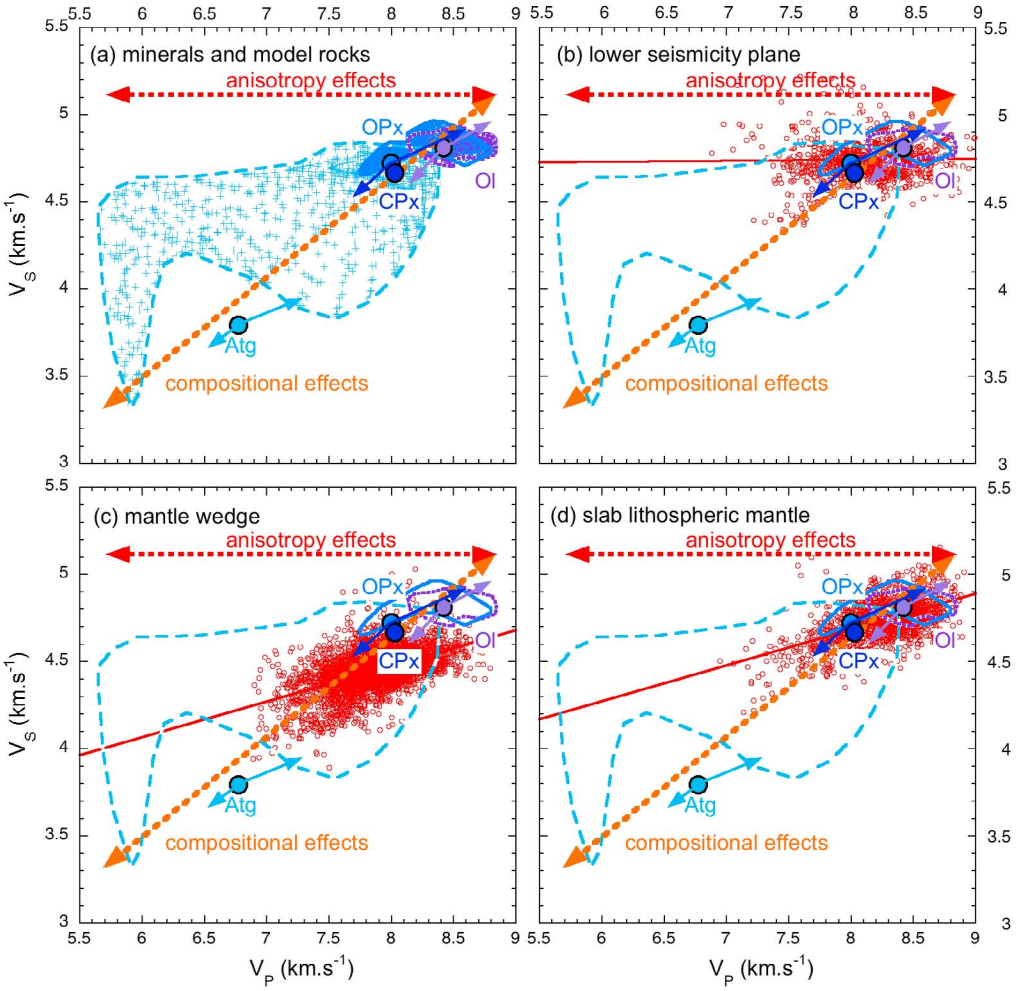

Figure 2. Seismic velocities in anisotropic mantle rocks and subduction. (a) Model mantle rocks and minerals from elastic data and CPO; only the fastest shear-wave branches (V_{S1}) sampled by arrival times used in the tomographic inversion were considered; purple symbols: olivine aggregate; blue symbols: average lithospheric mantle with olivine and orthopyroxene; light blue crosses: foliated serpentinite. Average isotropic values for olivine (Ol), orthopyroxene (OPx), clinopyroxene (CPx), and serpentine (Atg) are shown as large circles. Arrows indicate the effect of pressure (3 GPa) and temperature (600°C) on the individual minerals. (b) At the lower seismicity plane, observed seismic velocities (red symbols) match those of dry mantle rocks (blue and purple fields). The horizontal data dispersion (near zero slope of the linear regression) is due to anisotropy. (c) In the mantle wedge, the broad dispersion of seismic velocities along the diagonal is mostly due to temperature variations. (d) In the slab mantle between the lower plane and oceanic crust, the variability is intermediate and due both to temperature gradients of about 500K and to anisotropy.

V_P and V_S of 0.65 and 0.40 km.s^{-1}, respectively, for the lithospheric peridotite. Part of the variation may also be attributed to pressure variations, or to mixing of peridotites with serpentine layers observed at the top of the subduction [*Kawakatsu and Watada*, 2007; *Nakajima et al.*, 2009a] and imperfect separation with the oceanic crust layer (Figure S1).

[10] In the lithospheric mantle within the slab (Figure 2d), the variability is intermediate between that of the wedge and that of the lower seismicity plane. Temperatures vary here by about 500 K, resulting in expected variations of V_P and V_S of 0.33 and 0.20 km.s^{-1}, respectively. V_P has a larger variability than V_S, as reflected in the slope of the regression line that is intermediate between horizontal (anisotropy) and diagonal (composition, pressure, temperature). The effects of pressure and temperature on velocities nearly compensate each other and observed velocities are close to those calculated for peridotite at ambient conditions.

4. Anisotropic model for the slab mantle and lower seismicity plane in N-E Japan

[11] V_P anisotropy was modeled by considering two sources of deformation in the subducted lithospheric mantle (Figure 3). Firstly the original extension at mid-ocean ridge (MOR) produced fast axis alignment (N165) perpendicular to local magnetic lineation [*Shinohara et al.*, 2008; *Tono et al.*, 2009] that is bent by about 30° and 15° in the Hokkaido and Tohoku subduction, respectively. Secondly we assume that the fast V_P will align perpendicular to the trench in horizontal fault planes around the lower seismicity

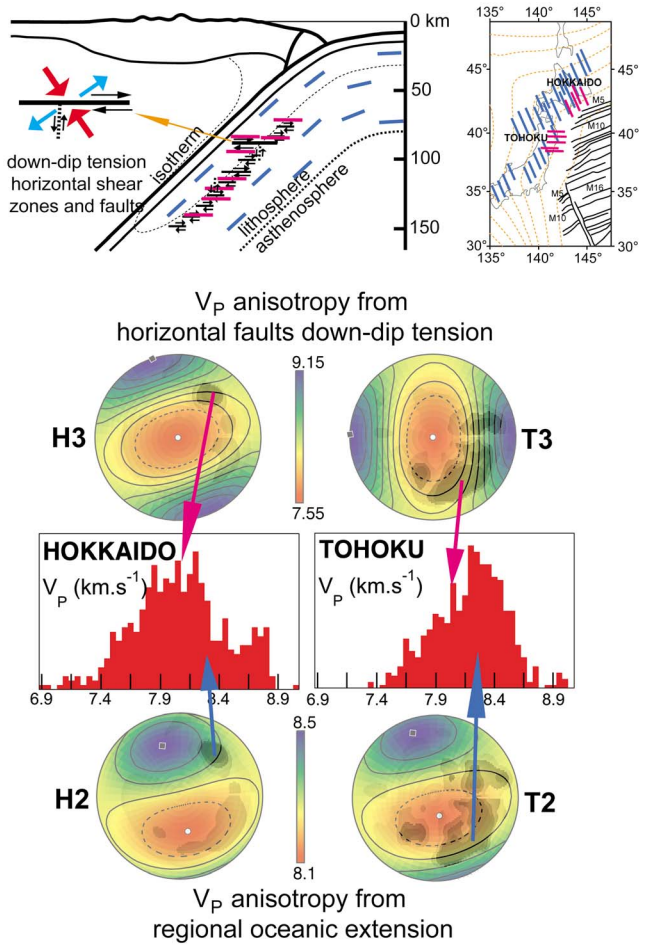

Figure 3. Anisotropy model of the lower seismicity plane. The schematic cross-section shows the planar horizontal faults with down-dip extension perpendicular to the trench consistent with focal mechanisms for lower seismicity plane and aftershock [*Kosuga et al.*, 1996]. This deformation results in alignment of fast V_P axis along the shear direction (magenta lines perpendicular to the trench). Small (about 10 km wide) faults form an array along the subduction. Larger (about 30 km) faults can yield large magnitude earthquake like the Kushiro-oki event (M=7.8) and associated low velocity anomaly (Figure 1). Slow axis is vertical. It is superimposed to weak regional anisotropy acquired during oceanic seafloor spreading (blue lines). Anisotropy azimuths are shown on the map. Stereographic projections of the corresponding V_P tensors are shown along with seismic ray distributions for specific points (Figure 1) in the lower plane and in the slab. The average V_P computed from ray direction statistics and anisotropy orientations (magenta and blue arrows) are shown by arrows pointing to the V_P histograms in the lower plane of Hokkaido and Tohoku region.

plane, in consistency with slab unbending direction, focal earthquake mechanisms [*Kosuga et al.*, 1996], and CPO of shear zones (type-A fabric [*Jung et al.*, 2006]) and pseudotachylites [*Jin et al.*, 1998]. The intersection of the ray orientations used for tomography with the stereographic projections of V_P tensor (Figure 3) for a given anisotropy orientation and strength gives the values of V_P for the rays emitted from the corresponding point in the tomographic cross section. The resulting V_P's are 8.0 and 8.3 km.s^{-1} for the lower plane and slab mantle at points H3 and H2 in Hokkaido, and T3 and T2 in Tohoku, respectively. Thus the difference in V_P accounts for the broad bimodal distribution on V_P histograms (Figure 3). Vertical faults would result in high velocities inconsistent with the observations.

5. Discussion

[12] The association of anisotropic peridotites with the lower seismicity plane proposed here does not require significant hydration of the mantle since anisotropic properties of anhydrous peridotites can well explain the observed seismic velocities. However seismic velocities alone are not sufficient to rule out the possibility of serpentinization. The low velocities areas of the lower seismicity plane are separated from the oceanic crust by slab lithospheric mantle with high average V_P of 8.25 and V_S of 4.7 km.s^{-1} that indicate insignificant serpentinization. Direct seismic observations of the hydrothermal serpentinization of the lithospheric mantle along faults due to slab bending at the trench are limited down to 2–3 km below oceanic crust [*Ranero et al.*, 2003]. Numerical models show that fluid infiltration due to bending decreases from top (oceanic crust) to bottom (mantle) and are likely limited to about 5 km [*Faccenda et al.*, 2009]. It would result in a decrease of serpentinization with increasing depths, and in an increase of velocities in the mantle from the oceanic crust down to the lower plane contrary to the observation.

[13] Dehydration embrittlement [*Peacock*, 2001] was proposed for the lower seismicity plane because the stability limits of serpentine at high pressure and temperatures between 550 and 670°C [*Ulmer and Trommsdorff*, 1995] match the thermal structure of subduction zones and account for larger DSZ separation in cold than in warm subductions [*Brudzinski et al.*, 2007]. The lower seismic plane of DSZ locates where stresses have built due to the unbending of subducted lithosphere 20–30 km below the oceanic crust [*Kawakatsu*, 1986] and may not require dehydration. Localized plastic deformation of peridotites in response to those stresses can ultimately result in seismic rupture via periodic shear instabilities occurring in a narrow 650–800°C interval consistent with lower plane temperature [*Kelemen and Hirth*, 2007].

[14] Plastic shearing of peridotites causes the alignment of the fast axis along the shear direction and of the slow axis perpendicular to the shear plane (type-A fabric typical of low temperatures [*Jung et al.*, 2006]). Beneath Hokkaido, a low-V_P anomaly is associated with a horizontal seismically active fault (Figure 1) where propagation of aftershocks of the 1993 Kushiro-oki earthquake has been observed [*Kosuga et al.*, 1996; *Nakajima et al.*, 2009b]. It supports the idea of a close link between plastic shearing, resulting seismic anisotropy and seismicity [*Kelemen and Hirth*, 2007]. Shear zones along the lower seismicity plane with different anisotropy than the surrounding lithospheric mantle are also imaged by V_P anisotropic tomography [*Wang and Zhao*, 2009]. Seismic strain rates for double seismic zones are estimated to be in the 0.2–2 10^{-15} s^{-1} range [*Kawakatsu*, 1986], yielding total strain of the order of 5% over the depth range where bending and unbending occur. Even if this strain is localized in a 5 km-wide zone around the lower

plane, it is possibly smaller (up to a few tens of %) than the value of about 100% required to cause significant anisotropy [*Kaminski and Ribe*, 2001]. If this interpretation is correct, it requires another source of deformation of the slab that would add up to slab bending and unbending. Precise thermo-mechanical modeling could resolve this issue.

[15] Low V_P and V_P/V_S ratio anomalies were also observed in association with the lower seismicity plane in the Chilean subduction zone [*Dorbath et al.*, 2008]. These low velocity patches are attributed to seismic anisotropy of deformed dry lithospheric mantle by analogy with the Pacific subduction beneath Japan, and not to serpentine as previously proposed [*Dorbath et al.*, 2008]. Similarly to the N–E Japan case, the low velocity anomalies of the Chilean lower seismicity plane are separated from the oceanic crust by high velocity regions typical of anhydrous mantle peridotites. Thus seismic anisotropy is observed in the lower plane of two subduction zones with different age and thermal regimes. If anisotropy and seismicity have a similar cause such as plastic deformation, anisotropy should be observed in the lower seismicity plane of most subduction zones since DSZ are a global feature [*Brudzinski et al.*, 2007].

[16] The preservation of a dry lithospheric mantle has consequences on the phase transformations taking place in the transition zone down the subduction zone. With water concentrations in olivine lower than 100 ppm since partial melting at the oceanic ridge has dried out the lithospheric mantle [*Karato and Jung*, 1998], it is possible to preserve metastable olivine wedges down to lower mantle depth in the core of cold slabs [*Diedrich et al.*, 2009; *Kubo et al.*, 2009] as observed under Japan [*Iidaka and Suetsugu*, 1992] and in the Mariana subduction [*Kaneshima et al.*, 2007]. Seismic observations from shallow to deep subduction are thus consistent with a dry lithospheric mantle that will not contribute significantly to water recycling except in the 2–3 km beneath the oceanic crust.

[17] **Acknowledgments.** This work benefited from the support of the ANR grant ANR-08-BLAN-0192 to BR. BR acknowledges support from University of Tokyo and ERI International Office during stays at the Earthquake Research Institute. Thoughtful comments from two anonymous reviewers helped to clarify the manuscript.

References

Abramson, E., J. Brown, L. J. Slutsky, and J. Zaug (1997), The elastic constants of San Carlos olivine to 17 GPa, *J. Geophys. Res.*, *102*(B6), 12,253–12,263, doi:10.1029/97JB00682.

Bezacier, L., B. Reynard, J. D. Bass, C. Sanchez-Valle, and B. V. Van de Moortele (2010), Elasticity of antigorite, seismic detection of serpentinites, and anisotropy in subduction zones, *Earth Planet. Sci. Lett.*, *289*(1–2), 198–208, doi:10.1016/j.epsl.2009.11.009.

Brudzinski, M. R., C. H. Thurber, B. R. Hacker, and E. R. Engdahl (2007), Global prevalence of double Benioff zones, *Science*, *316*(5830), 1472–1474, doi:10.1126/science.1139204.

Christensen, N. I. (2004), Serpentinites, peridotites, and seismology, *Int. Geol. Rev.*, *46*(9), 795–816, doi:10.2747/0020-6814.46.9.795.

Diedrich, T., T. G. Sharp, K. Leinenweber, and J. R. Holloway (2009), The effect of small amounts of H_2O on olivine to ringwoodite transformation growth rates and implications for subduction of metastable olivine, *Chem. Geol.*, *262*(1–2), 87–99, doi:10.1016/j.chemgeo.2009.01.011.

Dorbath, C., M. Gerbault, G. Carlier, and M. Guiraud (2008), Double seismic zone of the Nazca plate in northern Chile: High-resolution velocity structure, petrological implications, and thermomechanical modeling, *Geochem. Geophys. Geosyst.*, *9*, Q07006, doi:10.1029/2008GC002020.

Faccenda, M., T. V. Gerya, and L. Burlini (2009), Deep slab hydration induced by bending-related variations in tectonic pressure, *Nat. Geosci.*, *2*(11), 790–793, doi:10.1038/ngeo656.

Hasegawa, A., N. Umino, and A. Takagi (1978), Double-planed structure of deep seismic zone in northeastern Japan arc, *Tectonophysics*, *47*(1–2), 43–58, doi:10.1016/0040-1951(78)90150-6.

Iidaka, T., and D. Suetsugu (1992), Seismological evidence for metastable olivine inside a subducting slab, *Nature*, *356*, 393–395.

Isaak, D. (1992), High-temperature elasticity of iron-bearing olivines, *J. Geophys. Res.*, *97*(B2), 1871–1885, doi:10.1029/91JB02675.

Jackson, J. M., S. V. Sinogeikin, and J. D. Bass (2007), Sound velocities and single-crystal elasticity of orthoenstatite to 1073K at ambient pressure, *Phys. Earth Planet. Inter.*, *161*, 1–12, doi:10.1016/j.pepi.2006.11.002.

Jin, D., S. Karato, and M. Obata (1998), Mechanisms of shear localization in the continental lithosphere: Inference from the deformation microstructures of peridotites from the Ivrea zone, northwestern Italy, *J. Struct. Geol.*, *20*, 195–209, doi:10.1016/S0191-8141(97)00059-X.

Jung, H., I. Katayama, Z. Jiang, I. Hiraga, and S. Karato (2006), Effect of water and stress on the lattice-preferred orientation of olivine, *Tectonophysics*, *421*(1–2), 1–22, doi:10.1016/j.tecto.2006.02.011.

Kaminski, E., and N. Ribe (2001), A kinematic model for recrystallization and texture development in olivine polycrystals, *Earth Planet. Sci. Lett.*, *189*(3–4), 253–267, doi:10.1016/S0012-821X(01)00356-9.

Kaneshima, S., T. Okamoto, and H. Takenaka (2007), Evidence for a metastable olivine wedge inside the subducted Mariana slab, *Earth Planet. Sci. Lett.*, *258*(1–2), 219–227, doi:10.1016/j.epsl.2007.03.035.

Karato, S., and H. Jung (1998), Water, partial melting and the origin of the seismic low velocity and high attenuation zone in the upper mantle, *Earth Planet. Sci. Lett.*, *157*(3–4), 193–207, doi:10.1016/S0012-821X(98)00034-X.

Kawakatsu, H. (1986), Double seismic zones: Kinematics, *J. Geophys. Res.*, *91*(B5), 4811–4825, doi:10.1029/JB091iB05p04811.

Kawakatsu, H., and S. Watada (2007), Seismic evidence for deep-water transportation in the mantle, *Science*, *316*(5830), 1468–1471, doi:10.1126/science.1140855.

Kelemen, P. B., and G. Hirth (2007), A periodic shear-heating mechanism for intermediate-depth earthquakes in the mantle, *Nature*, *446*(7137), 787–790, doi:10.1038/nature05717.

Kosuga, M., T. Sato, A. Hasegawa, T. Matsuzawa, S. Suzuki, and Y. Motoya (1996), Spatial distribution of intermediate-depth earthquakes with horizontal or vertical nodal planes beneath northeastern Japan, *Phys. Earth Planet. Inter.*, *93*, 63–89, doi:10.1016/0031-9201(95)03089-1.

Kubo, T., S. Kaneshima, Y. Torii, and S. Yoshioka (2009), Seismological and experimental constraints on metastable phase transformations and rheology of the Mariana slab, *Earth Planet. Sci. Lett.*, *287*(1–2), 12–23, doi:10.1016/j.epsl.2009.07.028.

Mainprice, D. (1990), A FORTRAN program to calculate seismic anisotropy from the lattice preferred orientation of minerals, *Comput. Geosci.*, *16*(3), 385–393, doi:10.1016/0098-3004(90)90072-2.

Nakajima, J., Y. Tsuji, and A. Hasegawa (2009a), Seismic evidence for thermally-controlled dehydration reaction in subducting oceanic crust, *Geophys. Res. Lett.*, *36*, L03303, doi:10.1029/2008GL036865.

Nakajima, J., Y. Tsuji, A. Hasegawa, S. Kita, T. Okada, and T. Matsuzawa (2009b), Tomographic imaging of hydrated crust and mantle in the subducting Pacific slab beneath Hokkaido, Japan: Evidence for dehydration embrittlement as a cause of intraslab earthquakes, *Gondwana Res.*, *16*(3–4), 470–481, doi:10.1016/j.gr.2008.12.010.

Peacock, S. M. (2001), Are the lower planes of double seismic zones caused by serpentine dehydration in subducting oceanic mantle?, *Geology*, *29*(4), 299–302, doi:10.1130/0091-7613(2001)029<0299:ATLPOD>2.0.CO;2.

Pera, E., D. Mainprice, and L. Burlini (2003), Anisotropic seismic properties of the upper mantle beneath the Torre Alfina area (Northern Appennines, central Italy), *Tectonophysics*, *370*(1–4), 11–30, doi:10.1016/S0040-1951(03)00175-6.

Ranero, C. R., J. P. Morgan, K. McIntosh, and C. Reichert (2003), Bending-related faulting and mantle serpentinization at the Middle America trench, *Nature*, *425*(6956), 367–373, doi:10.1038/nature01961.

Reynard, B., N. Hilairet, E. Balan, and M. Lazzeri (2007), Elasticity of serpentines and extensive serpentinization in subduction zones, *Geophys. Res. Lett.*, *34*, L13307, doi:10.1029/2007GL030176.

Shinohara, M., T. Fukanoa, T. Kanazawa, E. Araki, K. Suyehiro, M. Mochizuki, K. Nakahigashi, T. Yamada, and K. Mochizuki (2008), Upper mantle and crustal seismic structure beneath the Northwestern Pacific Basin using a seafloor borehole broadband seismometer and ocean bottom seismometers, *Phys. Earth Planet. Inter.*, *170*, 95–106, doi:10.1016/j.pepi.2008.07.039.

Tono, Y., Y. Fukao, T. Kunugi, and S. Tsuboi (2009), Seismic anisotropy of the Pacific slab and mantle wedge beneath the Japanese islands, *J. Geophys. Res.*, *114*, B07307, doi:10.1029/2009JB006290.

Ulmer, P., and V. Trommsdorff (1995), Serpentine stability to mantle depths and subduction-related magmatism, *Science*, *268*(5212), 858–861, doi:10.1126/science.268.5212.858.

Wang, J., and D. P. Zhao (2009), P-wave anisotropic tomography of the crust and upper mantle under Hokkaido, Japan, *Tectonophysics*, *469* (1–4), 137–149, doi:10.1016/j.tecto.2009.02.005.

Webb, S. L., and I. Jackson (1993), The pressure dependence of the elastic moduli of single-crystal orthopyroxene ($Mg_{0.8}Fe_{0.2}$)SiO_3, *Eur. J. Mineral.*, *5*, 1111–1119.

H. Kawakatsu, Earthquake Research Institute, University of Tokyo, 1-1-1 Yayoi, Bunkyo-ku, Tokyo 113-0032, Japan.

J. Nakajima, Research Center for Prediction of Earthquakes and Volcanic Eruptions, Graduate School of Science, Tohoku University, 6-6 Aza-Aoba, Aramaki, Aoba-ku, Sendai 980-8578, Japan.

B. Reynard, Laboratoire de Sciences de la Terre, UMR 5570, Université de Lyon, CNRS, Ecole Normale Supérieure de Lyon, Site Monod, 15 parvis René Descartes, BP 7000, F-69342 Lyon CEDEX, France. (bruno.reynard@ens-lyon.fr)